Color Image Skeletonization: The Electrostatic Field-Based Approach

Tanya Grigorishin
Department of Computer Science
University of Saskatchewan
57 Campus Drive
Saskatoon, SK S7N 5A9
CANADA
e-mail: tpg134@cs.usask.ca

Supervisor: Yee-Hong Yang

Abstract

Skeleton representation of an object is a powerful shape descriptor that captures both boundary and region information of the object. The skeleton of a shape is a representation composed of idealized thin lines that preserve the connectivity or topology of the original shape. Although the literature contains a large number of skeletonization algorithms, many open problems remain.

In this paper, we present a skeletonization approach for color images that relies on the Electrostatic Field Theory (EFT). A surface color is represented in a 3-dimensional color space, from which boundary information is extracted prior to the skeletonization. We study two methods for the color boundary detection. The first algorithm uses color linearization by assigning a color similarity measure prior to the edge detection. The second performs a color edge detection before the boundary information is extracted. The performance of these boundary detection algorithms and the proposed EFT-based algorithm is studied extensively. The experimental results are encouraging.

Introduction

Shape representation and description is frequently used in most computer vision systems. A useful and reliable shape representation must meet a number of requirements, which include *invariance*, *uniqueness*, and *stability* (Mokhtarian & Mackworth 1986). If two objects have the same shape, then their representations should be the same and should be invariant with respect to translation, rotation, and scaling. Uniqueness means that if two objects have different shapes they should have different representations. Stability denotes the fact that if two objects have a small shape difference, then their representations should have a small difference. Conversely, if two representations have a small difference, then the objects they represent should also have a small shape difference. Therefore, a stable representation means one that is insensitive to noise. In short, the object shape and its representation should have a one-to-one correspondence property.

The representation should reflect the shape of an object at various levels of abstraction and should also combine both boundary and region information of the object. Finally, the shape descriptors and the recognition of objects should be efficiently computable. Other criteria for shape representation can be found in reference (Mokhtarian & Mackworth 1992).

The skeleton of a two-dimensional object is a transformation which maps the contour of the object into a one-dimensional line. A first systematic study of skeletons as introduced in (Blum 1967) meets most of the aforementioned requirements. Blum proposed the prairie fire model: if one applies fire to all the sides of P, and lets the fire propagate at constant speed, then the skeleton is the locus of points where fire fronts meet. The essence of skeletonization, as epitomized by the "grass-fire" method, is to find a connected, thin set of points that are equidistant from at least two different image boundary points. A formal definition is given in (Pavlidis & et al. 1982): "Let R be a plane set, B its boundary, and P a point in R. A nearest neighbor of P on B is a point M in B such that there is no other point in B whose distance from P is less than distance PM. If P has more than one nearest neighbor, then P is said to be a *skeletal point* of R. The union of all skeletal points is called the skeleton of R."

Since the introduction of the skeleton shape descriptor, many skeletonization algorithms have been reported in the literature (Smith 1987). Many problems, however, remain unsolved. For example, methods to quantitatively evaluate skeletons are still lacking. Recently, there are some efforts done in this direction (Lam & Suen 1992), (Lee, Lam, & Suen 1991), (Jaisimha & Haralick 1993).

Another problem with most skeletonization algorithms is their sensitivity to noise. Although there are many skeletonization algorithms, surprisingly little work has been directed towards studying their sensitivity to boundary noise. Also, some existing skeletonization approaches require that many parameters be supplied by the user (Leymarie & Levine 1992).

In this paper, a skeletonization approach for color images which is based on the Electrostatic Field Theory (EFT) for shapes with no holes is presented. The motivation of this research work stems from the following reasons. First, the encouraging results of a recently developed technique that uses EFT to determine a skeleton in a binary image. Secondly, EFT presents a natural solution for skeletonization that overcomes many problems associated with existing skeletonization techniques. In particular, connectivity, thinness, and other desirable features of a skeleton are guaranteed. Thirdly, EFT unifies notions of corner detection, thinning, skeletonization, and multiple scale representation of objects, all within the same framework.

The EFT-based approach for color images uses the boundary of an object in the image to perform skeletonization. Therefore, prior to skeletonization the color boundary detection is accomplished. Boundary detection has often used in many computer vision applications. For example, model based object recognition (Grimson & Lozano-Peres 1985), shape from motion computation (Ulman 1979), (Hildreth 1983) and stereo image analysis (Marr & Poggio 1979), (Grimson 1981). In this paper we study two color boundary detection techniques, and their influence on the skeletonization performed by the EFT-based method.

This paper is organized as follows. First, an overview of the related research in skeletonization and color boundary detection is presented. Two of color boundary detection algorithms have been studied in more detail. The proposed EFT-based approach is also presented and specific results can be found in Expreri-mental Results section. Finally, conclusions and future directions are discussed.

Related Work

This section gives a brief review of skeletonization algorithms along with their main characteristics and drawbacks. For a more complete survey of skeletonization algorithms the interested reader can consult reference (Smith 1987). We also provide an overview of existing color boundary detection techniques. The survey of color edge detection can be found in (Hildreth 1985).

Existing skeletonization approaches can be classified approximately into a small number of categories. The first category is based on *topological* or *direct thinning*. Thinning denotes the process of iteratively peeling away the object's contour pixels while preserving its topology (Lam, Lee, & Suen 1992). Many thinning techniques have been developed, including both sequential (Dill, Levine, & Noble 1987) and parallel (Guo & Hall 1992) algorithms. The drawbacks of thinning algorithms are noise sensitivity, loss of continuity, and distortion, which usually lead to counterintuitive results. Therefore, most thinning approaches have been directed towards character recognition applications. The reader may refer to reference (Lam, Lee, & Suen 1992) for a comprehensive survey and bibliography of thinning algorithms.

The second category is to compute the symmetric axes using *direct*, or *analytical* methods by approximating the object's boundary by a polygon. For noisy or biological (as cells) objects, this approximation leads to unavoidable inaccuracy. Algorithms belonging to this category are based on either heuristic methods (Martinez-Perez, Jimenez, & Navalon 1987),(Shapiro, Pisa, & Sklansky 1981) or more rigorous methods such as Vonoroi diagrams (Brandt & Algazi 1992), (Ogn-riewicz & Ilg 1992). Although this category has many advantages over thinning algorithms (since they make measurements of Euclidean distance in the continuous domain rather than in the digital grid), they are of little practical use mainly because of their computational complexity (for example, the Vonoroi diagram).

The third category of skeletonization algorithms is the *ridge following* algorithms. From the object shape, the *Distance Transform* (DT) is obtained, from which ridges are found. By the conventional ridge concept, ridge is a central elevated surface that rises sharply above two adjacent side surfaces. The projection of the extracted ridges from the DT map constitute the skeletal branches of the object. Ridges can be traced by the active contour model (Leymarie & Levine 1992) and by other methods (Gauch & Pizer 1992). Different DT's have been published in the literature. See (Leymarie & Levine 1992) for a survey. Algorithms in this category are relatively simple. In general, the skeletonization results of this category are more accurate and smoother than those of the other two categories (Leymarie & Levine 1992). However, the DT of an object is still sensitive to noise. Equidistance contours are as noisy as the boundary. Representative examples of this category can be found in (Danielsson 1980).

The proposed EFT-based approach has some commonalities with algorithms in the ridge following category, where the DT is replaced by an *electrostatic potential surface transform* and the ridge following process by the tracing of field lines passing through significant convexities and concavities detected along some equipotential contour. The proposed potential surface approach can represent the object's shape at different levels of smoothing or scale and can capture important shape information such as curvature. Furthermore, equipotential contours are smoother than equidistance contours which are employed in the ridge following category.

Many of the above mentioned thinning algorithms as well as the presented skeletonization technique, are edge-based methods that take distance or symmetry measures from image boundaries. Therefore, skeletonization can not be performed until color boundary detection is accomplished.

The grey-level edge detection, or intensity edge detection is usually sufficient to find most physical discontinuities in the scene. However, color is a useful characteristic for differentiating material changes from other types of scene discontinuities (Rubin & Richards 1985). These material changes are interesting because they outline object entities in the image, and are frequently used in object recognition. Most color edge detection techniques take place in several stages. The first stage is a color image boundary enhancement stage, and the subsequent stages link together discontinuities locations in the image (Sung 1992).

Color Boundary Detection

In this paper we use the RGB color vector space to represent color. This allows us to directly encode the red, green, and blue channel intensities of a color signal. Using this color representation model we have implemented two color boundary detection techniques which are discussed in the following subsections. We also study the noise sensitivity of these approaches. Noise can result in unwanted spurious edges or missing boundaries in edge maps. By noise in color signals we mean zero-mean gaussian noise with the same variance σ in each color channel.

Boundary Detection Using the Linearization Process

Figure 1 depicts the steps required to perform color boundary detection using the linearization process.

At the first stage we linearize color by assigning scalar similarity measure to colors in the color space. The following similarity measure ($\mathbf{S}_{\odot}$) is used:

$$\mathbf{S}_{\odot} = \frac{\mathbf{c} \odot \mathbf{c_R}}{|\mathbf{c}||\mathbf{c_R}|},$$

where $\odot$ stands for the vector dot product, $\mathbf{c}$ is the color vector being compared, and $\mathbf{c_R}$ is the reference "ridge" color. The similarity measure is a scalar that defines ridges of a certain "ridge" color. The "ridge" color is different for the ridges of a different color.

The next step is to perform differentiation (high pass spatial filtering or edge enhancement) operation by using the Sobel gradient operator. This operator uses two templates to enhance edges in the horizontal and vertical directions only. The user can select between two approximations of the true gradient: calculating the magnitude of the gradient by using squares and square roots (Euclidean distance evaluation), or by using absolute differences. The latter is computationally faster.

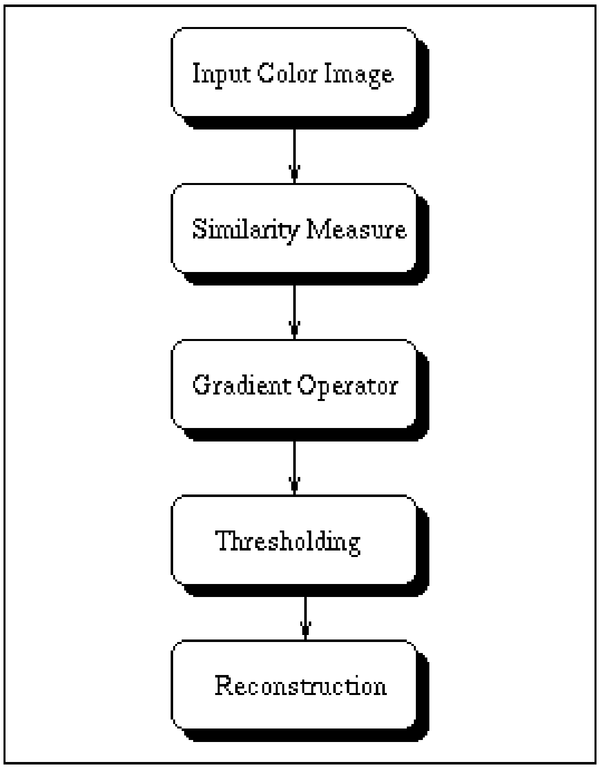

Figure 1: Color edge detection using the linearization process.

The process of edge detection leaves behind color edge segments that are generally well localized but mostly disconnected. The EFT-based skeletonization method requires the boundary of an object to be connected. Therefore, we extend and link together the disconnected edge segments to form continuous boundary output. This stage also discards false edge markings using some simple heuristics. The reader may consult to reference (Arumugam, Radhakrishnan, & Suen 1993) for a more detailed description of the adopted reconstruction of boundary segments.

Boundary Detection Using the Gradient Operator

This color boundary detection techniques is illustrated in Figure 2.

The first stage uses the gradient edge operator on a vector image field to enhance color discontinuities. Subsequent stages perform image thresholding and reconstruction of the edge map.

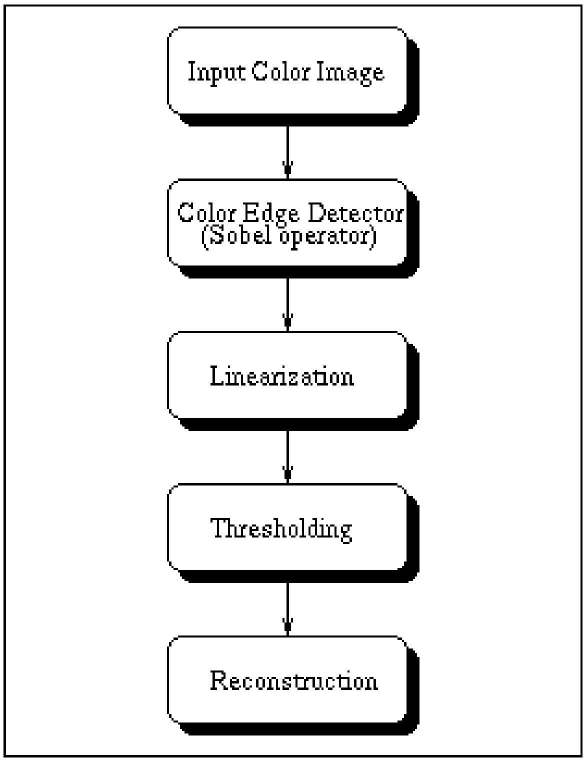

Figure 2: Color edge detection using the gradient operator.

Electrostatic Field-Based Approach to Skeletonization

The EFT-based skeletonization method models the boundary points found by a color boundary detector as unit charges, and their values are set to 1 (see Figure 3).

In the proposed approach, a skeleton is defined as following:

$$S = \{(x, y) \mid E(x, y) \text{ is a local maximum or minimum or } v(x, y) = 0\},$$

where $v(x, y)$ is the potential at the location (x,y) inside the object, and $E(x, y) = |\nabla v(x, y)|$ is the electrostatic field of the object. S represents the electrostatic field lines passing through points of significant convexities and concavities, and the points of zero potential. This definition differs from the conventional definition of a skeleton.

The following are the steps required to find the skeleton of a planar object:

1. Compute the potential distribution $V = v(x, y)$ inside the object,
2. Compute the electrostatic field in x and y directions: E_x and E_y, respectively,

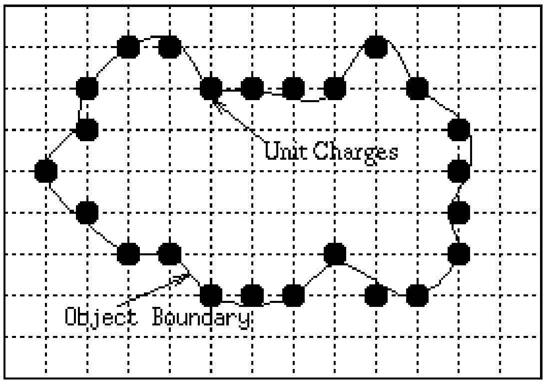

Figure 3: The model of the problem to generate the potential distribution on the object boundary.

3. Find the equipotential contour at a given potential v_{con},
4. Detect significant convexities and concavities along an equipotential contour, and
5. Trace skeletal points starting from points of significant convexities and concavities,

The following subsections give details of each of the above steps.

Solution of the Potential Distribution Inside the Object

The presented method of computation of the potential distribution inside the object uses a predefined structuring element. The structuring element K is as large as the image. The origin is at the center of the structuring element. The value of the element at location (x, y) is $\frac{1}{\sqrt{(x^2+y^2)}}$. It gives the contribution of a unit charge located at that location because the electrostatic potential $v(x, y)$ at the center is inversely proportional to the distance between (x, y) and the center of the mask. Hence, the total potential at the center of the mask is the summation of all the potentials due to charges within the neighborhood of the mask. The potential distribution is given by the convolution of K with the input image, which can be computed efficiently using the Fast Fourier Transform (FFT). The FFT of K is computed and then it is pointwise multiplied with the FFT of the input image. The inverse FFT is then performed to obtain the potential field distribution of the image.

After the potential distribution is computed, it is normalized as follows. The maximum potential of the object boundary is set equal to 255 and the minimum potential is set equal to 0. The potential values inside the object are computed using a simple linear transformation. The potential outside the object is set equal to 255.

The normalized map $V = v(x, y)$ is the potential surface of the object that is utilized for the construction of the skeleton. Figure 4 illustrates the potential surface generated for the image of a maple leaf.

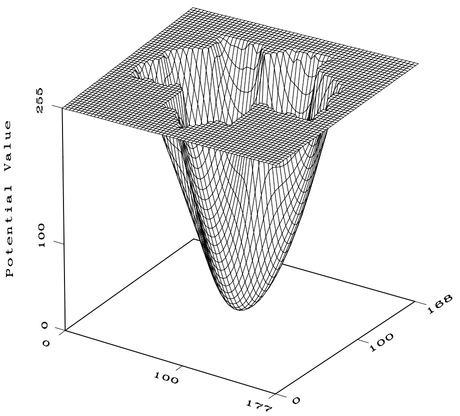

Figure 4: The potential surface generated for the image of a maple leaf.

Solution of the Electrostatic Field of the Object

The proposed approach for skeleton tracing uses the electrostatic field computed in x and y directions: E_x, and E_y, respectively. The computation for E_x, and E_y uses two structuring elements M_x and M_y. One for the x-direction, and one for the y-direction. The entries for the x-direction mask M_x are $-\frac{x}{r^3}$, where r is the distance from the center of the mask, similarly for the y-direction mask M_y the entries are $-\frac{y}{r^3}$. The electrostatic fields in the x-direction and the y-direction are given by the convolution with the M_x mask and the M_y mask, respectively. The computations of E_x, and of E_y are done using the FFT, similar to that for the computation of the potential distribution.

Construction of an Equipotential Contour at a Given Potential

The equipotential contour is used to detect significant convexities and concavities along the contour from which skeletal branches are initiated. This step can be visualized as a potential surface $V = v(x, y)$ being cut by a constant potential plane (parallel to the x-y plane). The curve that results from the intersection of the potential surface and the cutting plane is a closed contour.

The construction of a connected equipotential contour at a given potential, v_{con} within the range of 0 to 255, is based on the E_x, and E_y maps.

First, the starting point (x_0, y_0) of the equipotential contour, at which the potential is equal to v_{con}, is detected. Starting from this point, the equipotential contour is built at the subpixel resolution. It is well known that the equipotential contour is perpendicular to the field lines. Therefore the tracing direction of the contour is perpendicular to that given by the direction of the electrostatic field, which is specified by the $E_x(x, y)$ and $E_y(x, y)$ values. Thus, the next point (x_n, y_n) of the equipotential contour is chosen as following:

$$\begin{aligned} x_n &= x_{n-1} - E_y(x_{n-1}, y_{n-1}) \times \delta, \\ y_n &= y_{n-1} + E_x(x_{n-1}, y_{n-1}) \times \delta, \end{aligned}$$

where $E_x(x, y)$ and $E_y(x, y)$ are the electrostatic field values in x and y-directions at (x, y) location, respectively, and δ is the step size. In the implementation, δ is chosen to be 1 for all experiments. The result of this step is a one-dimensional curve $E(s)$ at the given potential v_{con}.

It is worth noting that the lower the value of the contour potential v_{con}, the smoother is the contour, the less the number of extrema of the field, and the less the number of significant convexities and concavities. This is expected due to the smoothing effect of the solution of the potential distribution inside the object.

From the above discussion, it is evident that the proposed skeletonization approach has the advantage of a multiscale approach. By appropriately choosing the equipotential contour at potential v_{con}, the desired level of details (or scale) of the skeleton can be selected. In particular, choosing an equipotential with a low value of v_{con}, a coarse skeleton is generated, whereas choosing an equipotential with a high value of v_{con}, a fine skeleton is generated. Such a smoothing effect has been used previously in reconstructing the three-dimensional default shape of an object from its occluding contour (Vega & Yang 1994). Figure 5 shows this interesting property of the potential distribution by depicting some equipotential contours of the maple leaf at various potentials.

Detecting Corners along the Equipotential Contour

Starting from the field distribution $E(s)$ along the contour s, convex (concave) corners are located by identifying points having local minima (maxima) of the field $E(s)$. As mentioned in the previous step, the choice of the contour potential v_{con} directly determines the degree of detail of the skeleton. Figure 6 demonstrates this fact by depicting different equipotential

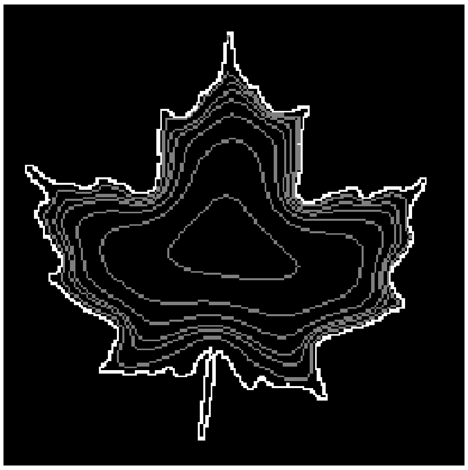

Figure 5: Smoothing effect and multiscale property of equipotential contours of the maple leaf. The bright contour is the boundary. The gray contours are the equipotential contours. The equipotential contours shown are constructed in the potential range 5-180 in steps of 15. When the contour is closer to the center of the object, the contour gets smoother and details tend to disappear.

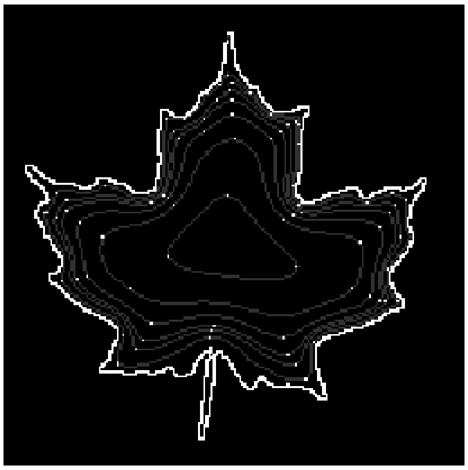

Figure 6: The equipotential contours and their associated corners (bright dots) of the maple leaf. The contours are constructed for the potential range 5-190 steps of 15. Notice that the number of corners increase with the potential v_{con}.

contours and their associated detected corners. The lower the potential, the lower the number of corners detected. Corners merging, disappearing, attracting, and repelling (Abdel-Hamid & Yang 1993) can be seen in the figure.

In this paper, both convex and concave corners are employed in generating skeletal branches.

Skeleton Tracing

Having identified points of significant convexities and concavities along an equipotential contour at a potential v_{con}, these points are used to initiate the skeleton tracing procedure. The skeleton branches correspond to field lines passing through significant corners identified in the previous step. Therefore, the skeleton generation procedure is reduced to the problem of tracing the field lines.

Starting from the points having significant convexities and concavities along an equipotential contour of potential v_{con}, the field lines are traced in two directions: in the inward direction (downhill generation) towards the object's central region or pixel, in the potential range $v_c = 0$, and in the outward direction (uphill generation) towards the object's boundary, in the potential range $v_b = 255$. Tracing is done in the direction defined by $E_x(x,y)$, $E_y(x,y)$, where $E_x(x,y)$ and $E_y(x,y)$ are the electrostatic field values in the x and y-directions at (x,y) location, respectively.

When tracing downhill the location of the next point x_n, y_n is defined at a subpixel resolution as following:

$$x_n = x_{n-1} - E_x(x_{n-1}, y_{n-1}) \times \delta,$$
$$y_n = y_{n-1} - E_y(x_{n-1}, y_{n-1}) \times \delta,$$

where δ is the step size. In the implementation, δ is chosen to be 1. The tracing process in inward direction terminates at the object's central pixel or at a region with a zero potential, at the global minimum potential.

The same process is used for the uphill generation towards the object's boundary. This process is terminated when the object's boundary is reached, i.e. reaching its global maximum energy.

It is noteworthy that the skeletal branches generated by this procedure is guaranteed to meet at the minimum potential region since the potential distribution decreases monotonically in the inward direction up to the potential. Also the connectivity requirement of the skeleton is guaranteed using this approach because the electrostatic field lines must be continuous.

Experimental Results and Discussion

A number of edge detection and skeletonization experiments have been conducted using both synthesized and real color images. Figure 7 illustrates the results obtained for a noise-free image using two examined color boundary detection techniques. The image size is 256×256. Figures 8 and 9 show the results of boundary detection for the leaf image corrupted with noise of level $\sigma = 8$ and $\sigma = 16$, respectively. The experimental results for the EFT-based skeletonization are demonstrated in Figures 10 - 12. Analyzing the presented

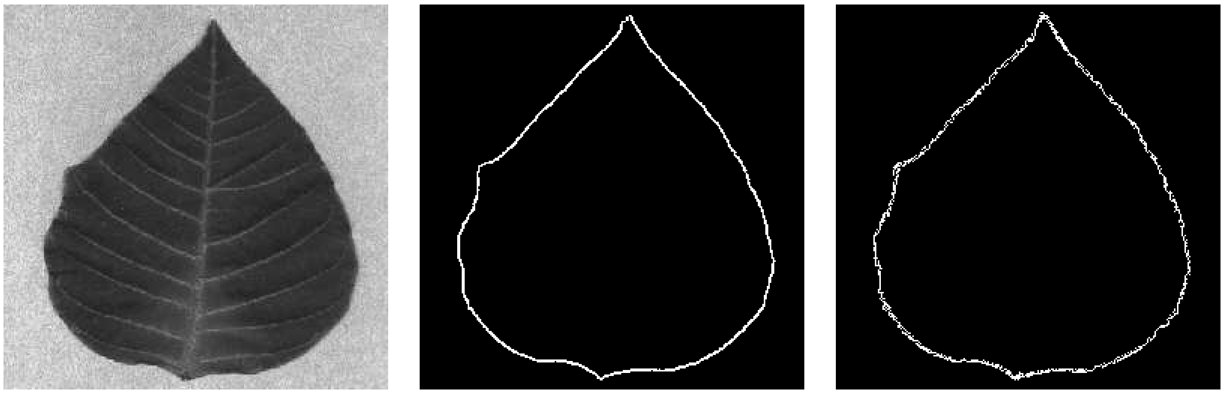

(a) (b) (c)

Figure 7: Boundary detection results. (a) Original color image; (b) Color boundary detection using the linearization process; (c) Color boundary detection using the gradient operator.

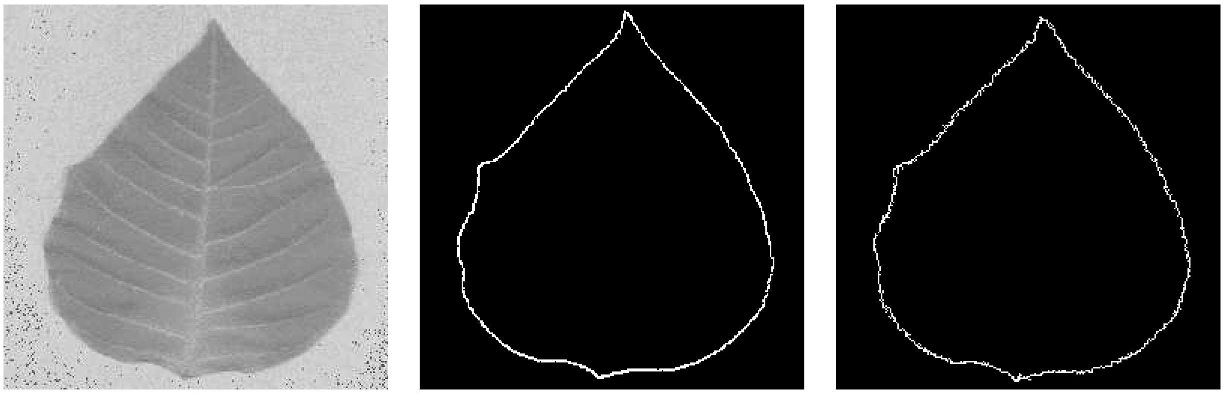

(a) (b) (c)

Figure 8: Noise boundary detection results. (a) Image of figure 7a corrupted with noise of level $\sigma = 8$; (b) Color boundary detection using the linearization process; (c) Color boundary detection using the gradient operator.

results, one can see that the EFT-based method is not highly dependent on the results of color boundary detection.

The proposed algorithm may be run with the option that the resultant skeletal points are labeled with their distance values to the object's boundary. Therefore, the original object can almost completely be recovered by means of a reverse-distance transformation (Arcelli & di Baja 1985). The Euclidean distance values are computed only for the skeletal points.

The connectivity and thinness requirements of the skeleton generated by the proposed approach are guaranteed, as explained above. Other thinning techniques do not always satisfy these requirements. Morphological thinning algorithm (Giardina & Dougherty 1988) does not give connected skeletons.

The above described color boundary detection techniques and the EFT-based skeletonization method were tested on a DEC alpha running OSF/1 V3.0. The algorithms are written in the C programming language. Tools in the Cantata visual programming environment were also employed (Cantata 1994).

The quantitative evaluation of the performance of color boundary detection algorithms in the presence of noise is presented in the following section.

Conclusions and Future Work

The problem of color edge detection and the influence of two edge detection techniques on the results of EFT-based skeletonization have been studied in this paper. The details of the steps that constitute the EFT-based skeletonization approach have been described. The approach has been shown to possess a number of desirable features that can naturally solve many problems that have challenged existing skeletonization approaches. First, connectivity and thinness are guar-

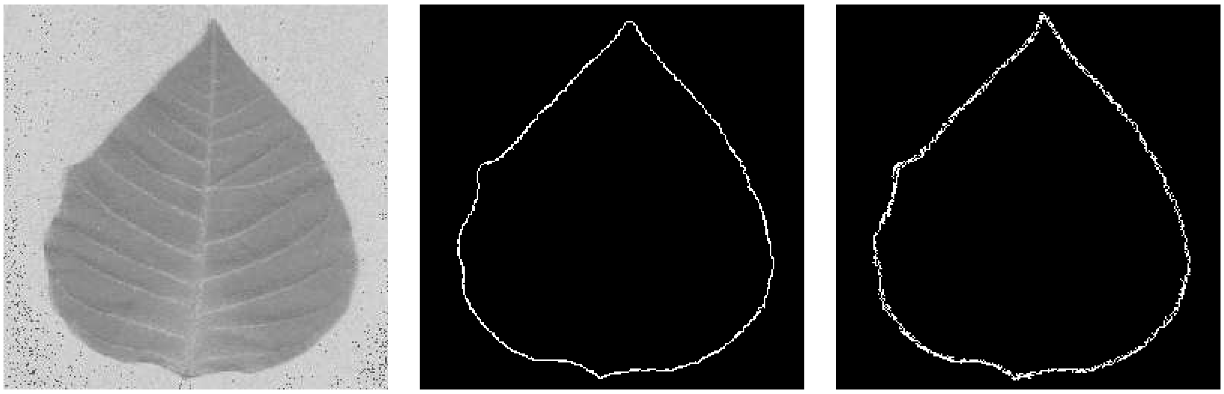

(a) (b) (c)

Figure 9: Noise boundary detection results. (a) Image of figure 7a corrupted with noise of level $\sigma = 16$; (b) Color boundary detection using the linearization process; (c) Color boundary detection using the gradient operator.

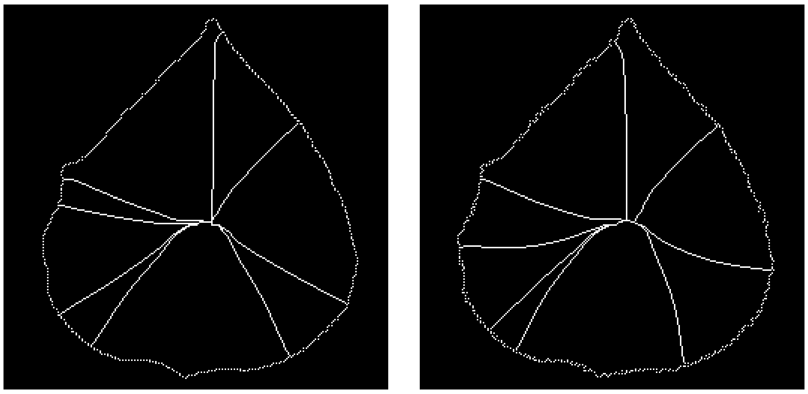

(a) (b)

Figure 10: Skeletons generated using EFT-based method for a noise-free image of the leaf. Skeletons started at equipotential contour 60. (a) Boundary image of Figure 7b is used in skeletonization; (b) Boundary image of Figure 7c is used in skeletonization;

anteed in the proposed approach. Secondly, the EFT-based approach gracefully captures and unifies notions of corner detection, multiscale representation, thinning, and skeletonization. Thirdly, the insensitivity of the proposed approach to severe boundary noise has been demonstrated experimentally. Experimentally we found that skeletonization does not require a high quality boundary detection results. Moreover, since the developed skeletonization approach is developed based on a well-established theory, the electrostatic field theory, the performance of the proposed approach under varying conditions can be predicted and justified before experiments are even conducted.

The potential distribution in its own constitutes a useful representation of objects at various levels of details similar to the multiscale curvature-based shape representation approach (Mokhtarian & Mackworth 1986), (Mokhtarian & Mackworth 1992). In the proposed approach, scale is naturally defined by the potential distribution. In fact, the equipotential contours generated from the potential surface can be viewed as fingerprints of the object (Piech 1988) for robust representation and recognition, the application of which is an interesting research topic.

Our research work using the EFT framework for solving computer vision problems inspires further research using the same approach in addressing other vision problems. A natural extension to the EFT-based approach is to use it in representing multidimensional objects. The potential surface becomes the *potential volume* and the equipotential contours are replaced by equipotential surfaces. This information can be possibly used to perform image segmentation and to accomplish skeletonization which does not require color boundary detection.

The experience in this work suggests that interest-

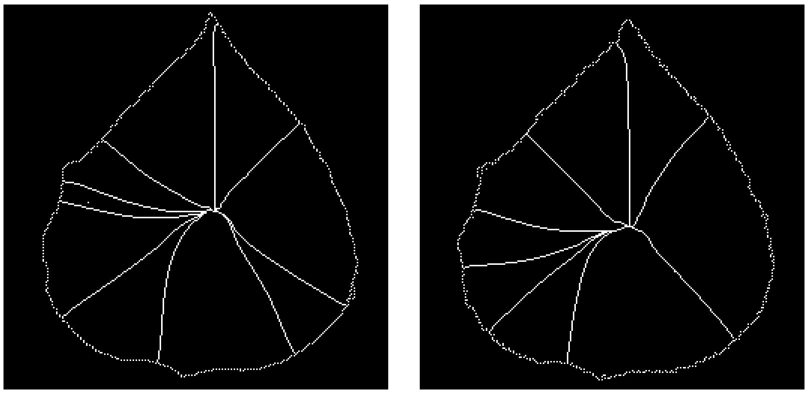

(a) (b)

Figure 11: Skeletons generated using EFT-based method for the image of a leaf corrupted with a noise of level $\sigma = 8$. Skeletons started at equipotential contour 50. (a) Boundary image of Figure 8b is used in skeletonization; (b) Boundary image of Figure 8c is used in skeletonization;

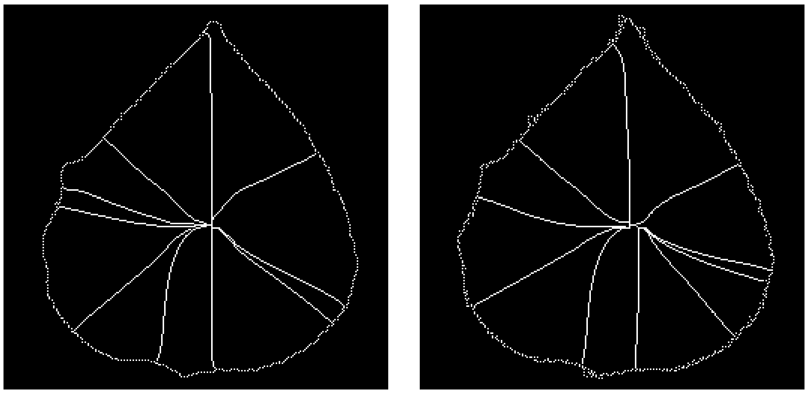

(a) (b)

Figure 12: Skeletons generated using EFT-based method from the image of a leaf corrupted with a noise of level $\sigma = 16$. Skeletons started at equipotential contour 45. (a) Boundary image of Figure 9b is used in skeletonization; (b) Boundary image of Figure 9c is used in skeletonization;

ing features exhibited by the electrostatic field-based approach of corner detection and skeletonization promote the investigation of more physics-based models in solving computer vision problems. Finally, it is believed that borrowing simple ideas from other disciplines, such as physics, will certainly benefit research in the computer vision community.

References

Abdel-Hamid, G. H., and Yang, Y. H. 1993. Electrostatic field-based detection of corners of planar curves. In *Proceedings of the 1993 Canadian Conference on Electrical and Computer Engineering, Vancouver, Canada*, 767–770.

Arcelli, C., and di Baja, G. S. 1985. A width independent fast thinning algorithm. *IEEE Transactions on Pattern Analysis and Machine Intelligence* 7:463–474.

Arumugam, A.; Radhakrishnan, T.; and Suen, C. Y. 1993. A thinning algorithm based on the force between charged particles. *Int. Journal of Pattern Recognition and Artifitial Intelligence* 7(5):988–1008.

Blum, H. 1967. A transformation for extracting new descriptors of shape. Technical report, MIT Press, Cambridge, MA.

Brandt, J. W., and Algazi, V. R. 1992. Continuous skeleton computation by vonoroi diagram. *CVGIP: Image Understanding* 55(3):329–338.

Cantata. 1994. *Krohos Research Inc.*

Danielsson, P. E. 1980. Euclidean distance mapping. *Computer Graphics and Image Processing* 14:227–248.

Dill, A. R.; Levine, M. D.; and Noble, P. B. 1987. Multiple resolution skeletons. *IEEE Transactions on Pattern Analysis and Machine Intelligence* 9:495–504.

Gauch, J., and Pizer, S. 1992. The intensity axis of symmetry and its application to image segmentation. *IEEE Transactions on Pattern Analysis and Machine Intelligence* 15(8):753–770.

Giardina, C. R., and Dougherty, E. 1988. *Morphological Methods in Image and Signal Processing.* Prentice-Hall.

Grimson, W. E., and Lozano-Peres, T. 1985. Model-based recognition from sparse range data. In *Techniques for 3-D Machine Perception, North-Holland, Amsterdam.*

Grimson, W. E. 1981. *From Images To Surfaces.* MIT Press, Cambrigde, MA.

Guo, Z., and Hall, R. W. 1992. Fast fully parallel thinning algorithms. *CVGIP: Image Understanding* 55(3):317–328.

Hildreth, E. C. 1983. *The Measurement of Visual Motion.* MIT Press, Cambrigde, MA.

Hildreth, E. C. 1985. Edge detection. Technical report, Artificial Intelligence Laboratory, MIT, Cambridge, MA.

Jaisimha, M. Y., and Haralick, R. M. 1993. A methodology for the characterization of the performance of thinning algorithms. *ICDAR* 282–286.

Lam, L., and Suen, C. Y. 1992. Automatic evaluation of skeleton shapes. In *Proc. 11th Int. Conference on Pattern Recognition, The Haque, The Netherlands*, 342–345.

Lam, L.; Lee, S. W.; and Suen, C. Y. 1992. Thinning methodologies - a comprehensive survey. *IEEE Transactions on Pattern Analysis and Machine Intelligence* 14(9):869–885.

Lee, S. W.; Lam, L.; and Suen, C. Y. 1991. Performance evaluation of skeletonization algorithms for document image processing. In *Proc. 1st Int. Conference on Document Analysis and Recognition, St. Malo, France*, 260–271.

Leymarie, F., and Levine, M. D. 1992. Simulating the grassfire transform using an active contour model. *IEEE Transactions on Pattern Analysis and Machine Intelligence* 14(1):56–75.

Marr, D., and Poggio, T. 1979. A theory of human stereo vision. In *Proc. of Royal Society of London B*, volume 204, 321–328.

Martinez-Perez, M. P.; Jimenez, J.; and Navalon, J. L. 1987. A thinning algorithm based on contours. *Computer Graphics and Image Processing* 39:186–201.

Mokhtarian, F., and Mackworth, A. K. 1986. Scale-based description and recognition of planar curves and two-dimensional shapes. *IEEE Transactions on Pattern Analysis and Machine Intelligence* 8(1):34–43.

Mokhtarian, F., and Mackworth, A. K. 1992. A theory of multiscale, curvature-based shape representation for planar curves. *IEEE Transactions on Pattern Analysis and Machine Intelligence* 14(8):789–805.

Ognriewicz, R., and Ilg, M. 1992. Vonoroi skeletons: Theory and applications. In *Proc. IEEE Conference on CVPR, Champaign, Illinois*, 63–69.

Pavlidis, T., and et al. 1982. Algorithm for graphics and image processing. *Computer Science Press.*

Piech, M. A. 1988. Comment on fingerprints of two-dimensional edge models. *Computer Vision, Graphics and Image Processing* 42:381–386.

Rubin, J. M., and Richards, W. A. 1985. Colour vision and image intensities: When changes material. Technical report, Artificial Intelligence Laboratory, MIT, Cambridge, MA.

Shapiro, B.; Pisa, J.; and Sklansky, J. 1981. Skeleton generation from x, y boundary sequences. *Computer Graphics and Image Processing* 15:136–153.

Smith, R. W. 1987. Computer processing of line images: A survey. *Pattern Recognition* 20(1):7–15.

Sung, K. K. 1992. A vector-signal processing approach to color. Master's thesis, MIT, Cambridge, MA.

Ulman, S. 1979. *The Interpretation of Visual Motion.* MIT Press, Cambrigde, MA.

Vega, O. E., and Yang, Y. H. 1994. Default shape theory: with application to the computation of the direction of the light source. *CVGIP: Image Understanding* 60(3):285–299.